Available online at www.sciencedirect.com
ScienceDirect
Thermochimica Acta 451 (2006) 84–93
thermochimica acta
www.elsevier.com/locate/tca

Structural, redox and acid–base properties of V_2O_5/CeO_2 catalysts

Xiaodong Gu [a], Jiazhen Ge [a], Huiliang Zhang [a], Aline Auroux [b], Jianyi Shen [a,*]

[a] *Laboratory of Mesoscopic Chemistry, School of Chemistry and Chemical Engineering, Nanjing University, Nanjing 210093, China*
[b] *Institute de Recherches sur la Catalyse, CNRS, 2 Avenue Albert Einstein, 69626 Villeurbanne Cedex, France*

Received 17 July 2006; received in revised form 14 September 2006; accepted 14 September 2006
Available online 19 September 2006

Abstract

CeO_2 supported V_2O_5 catalysts were prepared by the wetness impregnation technique and their surface structures were characterized by O_2 chemisorption, X-ray diffraction (XRD) and Raman spectroscopy (LRS). The surface acidity and basicity were measured by using microcalorimetry and infrared spectroscopy (FTIR) for the adsorption of NH_3 and CO_2. Temperature programmed reduction (TPR) was employed for the redox properties. In particular, isopropanol probe reactions with and without the presence of O_2 were employed to provide the additional information about the surface acidity and redox properties of the catalysts. Variation of loading of V_2O_5 and calcination temperature brought about the changes of surface structures of dispersed vanadium species, and hence the surface acidic and redox properties. Structural characterizations indicated that V_2O_5 can be well dispersed on the surface of CeO_2. The monolayer dispersion capacity was found to be about 8 V/nm^2, corresponding to about 10% V_2O_5 by weight in a V_2O_5/CeO_2 sample with the surface area of 80 m^2/g. Vanadium species in the catalysts (673 K calcined) with loading lower than 10% were highly dispersed and exhibited strong surface acidity and redox ability, while higher loading resulted in the formation of significant amount of surface crystalline V_2O_5, which showed fairly strong surface acidity and significantly weakened redox ability. Calcination of a 10% V_2O_5/CeO_2 at 873 K resulted in the formation of mainly $CeVO_4$ on the surface, which showed low surface acidity and redox ability. The probe reaction seemed to suggest that the calcination at higher temperature might cause the decrease of surface acidity more than redox ability. Thus, the 10% V_2O_5/CeO_2 catalyst calcined at 873 K exhibited much higher selectivity to benzaldehyde as compared to other V_2O_5/CeO_2 catalysts studied in this work, although its activity for the conversion of toluene was relatively low.

Keywords: V_2O_5/CeO_2 catalyst; Structural characterization; Surface acidity; Surface redox property; Isopropanol probe reactions; Selective oxidation of toluene

1. Introduction

Supported vanadia are extensively used as industrial catalysts for the processes such as selective oxidation of methanol to formaldehyde [1] and methyl formate [2], selective oxidation of *o*-xylene to phthalic anhydride [3,4], ammoxidation of alkyl aromatic hydrocarbons [5,6], removal of NO_x and SO_x [7], oxidation of SO_2 to SO_3 [8], selective catalytic reduction (SCR) of nitric oxides [9], etc.

Due to the restrictions of thermal stability, mechanical strength and surface area of bulk V_2O_5, it is generally not used directly as a catalyst in industry. It is usually supported on different carriers for different purposes. With a suitable support, its surface area, thermal stability and mechanical strength could be improved [10]. Studies indicated that the intensive interactions between a support and V_2O_5, and the dispersion and surface structures as well as the redox and acid–base properties of V_2O_5 would be modified by supports [11,12]. Hence, the supported V_2O_5 are sometimes used as model catalysts [13]. In fact, by employing different supports (such as SiO_2, Al_2O_3 and TiO_2) and loadings, the surface structure [14,15] and number of surface sites as well as the surface acid–base [16–18] and redox properties [19] can be intentionally monitored.

Due to its prominent ability of storing and feeding oxygen, CeO_2 has attracted much attention by the researchers in catalysis [20] with the emphasis on CeO_2 supported noble metals used in the auto-exhaust treatments [21]. There were a few studies reported for the system of V_2O_5/CeO_2. Courcot et al. [22,23] found that $CeVO_4$ was formed due to the reaction between V_2O_5 and CeO_2 at high temperatures. Knözinger et al. [24] used V_2O_5/CeO_2 catalysts for the dehydrogenation of propane and obtained some good results.

In this work, we studied the V_2O_5/CeO_2 catalysts mainly in terms of their surface acid–base and redox properties which

* Corresponding author. Tel.: +86 25 83594305; fax: +86 25 83317761.
E-mail address: jyshen@nju.edu.cn (J. Shen).

0040-6031/$ – see front matter © 2006 Elsevier B.V. All rights reserved.
doi:10.1016/j.tca.2006.09.007

were attempted to be correlated with the catalytic behavior of these catalysts for the selective oxidation of toluene to benzaldehyde and benzoic acid. Specifically, the surface acidity and basicity were characterized by employing the microcalorimetric adsorption of ammonia and CO_2, while the redox property was revealed by the traditional technique of temperature-programmed-reduction (TPR). Meanwhile, the surface acidity/basicity and redox property as well as their relative importance were probed by the reaction of isopropanol over the catalysts with and without the presence of O_2.

2. Experimental

2.1. Sample preparation

CeO_2 was obtained by calcining $Ce(NO_3)_2{\cdot}6H_2O$ (A.R.) in air at 773 K for 5 h. The V_2O_5/CeO_2 catalysts with various loadings (2.5–20 wt.% V_2O_5) were prepared by using the wetness impregnation method. Specifically, in each case of preparation, a known amount of CeO_2 was added into the aqueous solution containing the desired amount of vanadium oxalate and stirred. After being kept at room temperature overnight, it was dried at 383 K for 12 h and then calcined at 673 K for 5 h. One sample (10% V_2O_5/CeO_2) was also calcined separately at 773 and 873 K for 5 h, and was termed as 10% V_2O_5/CeO_2 (773 K) and 10% V_2O_5/CeO_2 (873 K), respectively. A bulk V_2O_5 was prepared for comparison by calcining a NH_4VO_3 (A.R.) at 673 K for 5 h.

2.2. Characterizations

Surface areas (S_{BET}) of the samples were measured on the Micromeritics ASAP 2000 instrument employing the BET method. The samples were degassed at 623 K for 2 h and N_2 adsorption was performed at 77 K.

The dispersion of vanadium species was measured by using the high temperature oxygen chemisorption method (HTOC) [25]. A sample was reduced in flowing H_2 at 640 K for 2 h, and then oxygen uptake was measured at the same temperature.

The X-ray diffraction (XRD) was performed on a Swiss made X'TRA X-ray diffractometer using a Cu target with radiation of 0.15418 nm and a scanning speed of 10°/min. The applied voltage and current were 45 kV and 40 mA, respectively.

Raman spectra (LRS) were collected on a France made JY HR800 spectrograph with a resolution of 2 cm^{-1}.

X-ray photoelectron spectra (XPS) were acquired with a Britain VG ESCALB MK-II using Mg Kα (1253.6 eV) as the excitation source and C 1s (284.6 eV) as the internal standard. The surface atomic ratio was obtained by the integral comparison of the element peak areas.

Microcalorimetric adsorption measurements were performed by using a Setaram C80 calorimeter. The samples were calcined in 500 Torr O_2 at 673 K for 1 h followed by evacuation at 673 K for 2 h. NH_3 and CO_2 were used as the probe molecules for the measurements of surface acidity and basicity, respectively. The probe molecules were purified with the freeze–pump–thaw cycles. Microcalorimetric adsorption measurements were carried out at 423 K.

The infrared (FTIR) measurements for NH_3 adsorbed samples were recorded with a Bruker IFS66V FTIR spectrograph. The samples were self-sustaining wafers with 13 mm in diameter and a thickness of about 20 mg/cm^2. A wafer was usually treated in 500 Torr O_2 at 673 K for 1 h, followed by evacuation for 2 h. About 10–20 Torr NH_3 was introduced and then evacuated at room temperature after 30 min. The IR spectra of the surface species were obtained by subtracting the blank from the spectra with adsorbed ammonia.

The TPR apparatus used was a home-made unit. The hydrogen consumption peak was monitored by a thermal conductivity detector (TCD). The sample holder was a U-tube made of quartz (Ø3). A 5% H_2/N_2 gas mixture with a purity of 99.999% was used for the TPR with a flow rate of 40 mL/min. In each measurement, about 50 mg of a sample was used. After sweeping with the 5% H_2/N_2 mixed gas for 0.5 h at room temperature, the temperature was raised linearly with a rate of 10 K/min.

2.3. Catalytic tests

The dehydration and dehydrogenation reactions of isopropanol were carried out in a home-made fixed-bed microreactor (Ø12) connected to a gas chromatograph. The samples were heated in air at 673 K for 1 h before the reaction. The carrier gas (N_2 or air) with a flow rate of 60 mL/min was passed through a liquid saturator containing isopropanol at 295 K, when isopropanol was evaporated and passed through the catalyst bed at a rate of 3 mL/min (in vapor). About 0.1 g of a sample (20–40 meshes) was loaded for each test. The data were usually collected after the reaction for 2 h when the stable state was achieved. The reaction products were analyzed on-line with gas chromatograph using a packed column PEG 20000 and a flame ionization detector (FID).

The catalytic oxidation of toluene was performed in a fixed-bed micro-reactor (Ø10) connected to a gas chromatograph. Air with a flow rate of 62 mL/min was passed through a liquid saturator containing toluene at 330 K in order to have a molar ratio of air to toluene of 5:1. About 0.5 g catalyst (20–40 meshes), diluted with 2 mL quartz sand (20–40 meshes), was loaded for each test. The catalysts were usually treated in air at 673 K for 1 h before the reaction. The reaction temperature was monitored at 623 K and the reaction data were collected after 2 h in stream when the stable state was achieved. The reaction products were analyzed on-line with a gas chromatograph. A capillary column (HP-FFAP) with a FID was used to detect toluene, benzaldehyde, benzoic acid, benzoic alcohol and other possible organic products while a packed column (Hayesep D) with a TCD was used to detect CO and CO_2.

3. Results and discussion

3.1. Surface structures

The surface areas of the catalysts were given in Table 1. The support, CeO_2, obtained by the direct calcination of

Table 1
Surface area, O_2 uptake, density of adsorbed O, and calculated density of V on the surface of V_2O_5/CeO_2 catalysts

Catalyst	S_{BET} (m^2/g)	O_2 uptake[a] (mmol/g)	O density measured[b] (O/nm^2)	V density calculated[c] (V/nm^2)
CeO_2	83	0.119	1.73	0
2.5% V_2O_5/CeO_2	81	0.198	2.94	2.04
5% V_2O_5/CeO_2	72	0.303	5.07	4.60
10% V_2O_5/CeO_2	56	0.373	8.02	11.83
10% V_2O_5/CeO_2 (773 K)	45	0.292	7.82	14.72
10% V_2O_5/CeO_2 (873 K)	26	0.120	5.56	25.47
20% V_2O_5/CeO_2	48	0.372	9.34	27.60
V_2O_5	14	0.270	23.23	473.1

[a] Both reduction of samples by H_2 and O_2 adsorption were performed at 640 K.
[b] Supposing that each surface V adsorbs an oxygen atom.
[c] Supposing that all the vanadium atoms locate on the surface (100% dispersion).

$Ce(NO_3)_3{\cdot}6H_2O$ had a BET area of 83 m^2/g. With the addition of V_2O_5, the surface area was decreased with the increase of loading. There are usually two reasons responsible for the decrease of surface area of supported catalysts: (1) some pores are blocked by the supported species [26] and (2) solid reaction may occur between the support and supported species to form some new compound that is of low surface area [22,23]. In the present work, the calcination temperature (673 K) was lower than that for the solid reaction between CeO_2 and V_2O_5, and the decrease of surface area might be ascribed to the reason (1). For the 10% V_2O_5/CeO_2, surface area was decreased from 56 to 26 m^2/g when the calcination temperature was increased from 673 to 873 K. This was apparently due to the solid reaction. In fact, we will show later that a new compound, $CeVO_4$, was formed when the 10% V_2O_5/CeO_2 was calcined at higher temperatures. The V_2O_5 used in this work was obtained by the direct calcination of NH_4VO_3 and its surface area was determined to be 14 m^2/g.

The monolayer dispersion capacity for V_2O_5 can be calculated theoretically [27]. However, the dispersion strongly depends on the method of preparation and properties of interactions between the support and supported species. V_2O_5 may not be dispersed monolayerly even if the loading is lower than the monolayer dispersion capacity. For V_2O_5/CeO_2, the situation might be even more complicated since a solid reaction would occur. Therefore, we prepared the catalysts with different loadings (2.5–20%) and calcined one of them (10%) at different temperatures (673, 773 and 873 K) in order to investigate the factors influencing the dispersion and surface structure of V_2O_5 on CeO_2.

O_2 adsorption can be used to titrate the dispersion of a metal oxide on the surface of a support. Parekh and Weller [28] and Weller [29] proposed a low temperature oxygen adsorption method (LTOC) while Oyama et al. [25] suggested a high temperature oxygen adsorption method (HTOC). It was also suggested that the HTOC might pose less possibility for the bulk reduction and sintering [30], and therefore, we adopted this method for the measurements of vanadium dispersion in this work. Table 1 gives the density of surface oxygen atom obtained in this way. Different from the supports such as Al_2O_3, SiO_2 and TiO_2, CeO_2 itself adsorbed a large amount of O_2, indicating that some Ce^{4+} were reduced to Ce^{3+} in H_2 at 640 K. Addition of V_2O_5 increased the O_2 uptake, and reached a maximum (0.373 mmol/g) at the loading of 10%. Further increase of V_2O_5 loading did not increase the O_2 uptake, indicating that the amount of V_2O_5 in 10% V_2O_5/CeO_2 might have reached or even exceeded the monolayer dispersion capacity. For the 10% V_2O_5/CeO_2, calcination at higher temperatures decreased O_2 uptake, probably due to the decreased surface area or the formation of $CeVO_4$ that is more resistant to reduction and oxidation.

The surface oxygen density (SOD) measured varied with V_2O_5 loading, too. It increased significantly from 1.73 to 8.02 O/nm^2 with the loading up to 10%. Further increase of loading did not increase SOD significantly, again indicating the reach of the monolayer capacity. For the 10% V_2O_5/CeO_2, calcination at higher temperatures greatly decreased the O_2 uptake. However, the decrease of SOD was not as great as that of O_2 uptake. This might be due to the decrease of surface area upon calcination at higher temperatures. It is interesting to note that the 10% V_2O_5/CeO_2 (673 K) and 10%V_2O_5/CeO_2 (773 K) had the similar SOD (8.02 O/nm^2 versus 7.82 O/nm^2), indicating some similarities of surface structure of vanadium species in these two samples. Calcination at 873 K greatly decreased SOD, implying the formation of some compound with low redox ability.

Since the reduced CeO_2 also adsorbed O_2, it was difficult to estimate the surface V density (SVD) by supposing the 1/1 ratio for O/V. When the loading of V_2O_5 was low, oxygen must adsorb on both V and Ce sites. With the increase of loading, the surface CeO_2 might be covered by V_2O_5 and oxygen might be adsorbed mainly on V sites. By comparing SOD measured with SVD calculated supposing 100% dispersion of V_2O_5, it is clearly seen from Table 1 that the measured SOD was greater than SVD for the samples with 2.5% and 5% V_2O_5, indicating that the O_2 adsorption did occur on both V and Ce sites. In contrast, with the further increase of loading, the measured SOD was lower than calculated SVD, implying that O_2 adsorption occurred mainly on V sites. In this case, it seems possible to estimate the dispersion of V_2O_5. Suppose that oxygen adsorption only involved V sites for the 10% V_2O_5/CeO_2 (673 K), the dispersion of V_2O_5 was estimated to be about 68%. In addition, the surface V density of this sample was about 8 V/nm^2 as determined by O_2 adsorption (supposing O/V = 1). The monolayer capacity can then be estimated to be 6.8% V_2O_5 with the surface area of 56 m^2/g. Ten percent V_2O_5 should be the

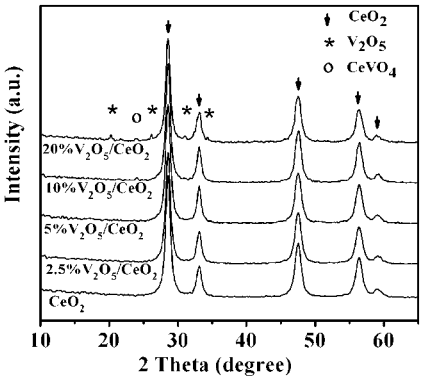

Fig. 1. XRD patterns of V_2O_5/CeO_2 catalysts.

monolayer capacity for a V_2O_5/CeO_2 sample with the surface area of 80 m^2/g. Thus, the vanadia loading in 10% V_2O_5/CeO_2 (673 K) (56 m^2/g) exceeded the monolayer capacity. The SOD measured for unsupported V_2O_5 was 22.23 O/nm^2, which was much higher than the theoretical value of 8 O/nm^2, indicating that the HTOC method might have titrated some bulk V_2O_5. The SODs measured for the 10% V_2O_5/CeO_2 (873 K) and 20% V_2O_5/CeO_2 were about 21.8% and 33.8% of those of calculated SVDs, owing to the formation of $CeVO_4$ and crystalline V_2O_5 on the surface, respectively.

Fig. 1 gives the XRD patterns of V_2O_5/CeO_2 catalysts with different loadings. All the samples exhibited the characteristic peaks of CeO_2. XRD patterns for $CeVO_4$ appeared for the 10% V_2O_5/CeO_2 and 20% V_2O_5/CeO_2 samples. Knözinger et al. suggested that VO_x and CeO_2 began to react to form $CeVO_4$ on the surface at 573 K [24]. With the increase of loading, crystalline V_2O_5 appeared in the 20% V_2O_5/CeO_2 sample. No XRD patterns for crystalline V_2O_5 and $CeVO_4$ were observed for the samples with the loading of V_2O_5 lower than 10%, indicating the highly dispersed states of vanadium species in these samples.

Fig. 2 shows the XRD patterns for the 10% V_2O_5/CeO_2 calcined at different temperatures. The characteristic peaks for $CeVO_4$ became more intensive and sharper with the increase of calcination temperature, illustrating the formation of more $CeVO_4$ and the growth of its particle size. Meanwhile, the peaks for CeO_2 also became sharper, indicating the sintering of CeO_2, which was consistent with the results of measurements of surface areas and O_2 adsorption.

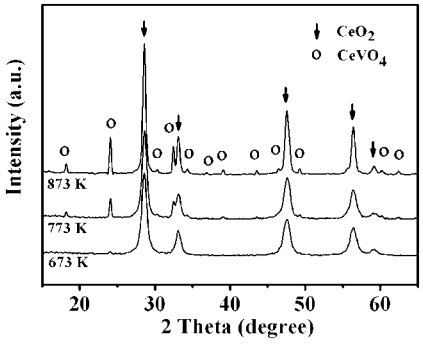

Fig. 2. XRD patterns of the 10% V_2O_5/CeO_2 catalyst calcined at different temperatures.

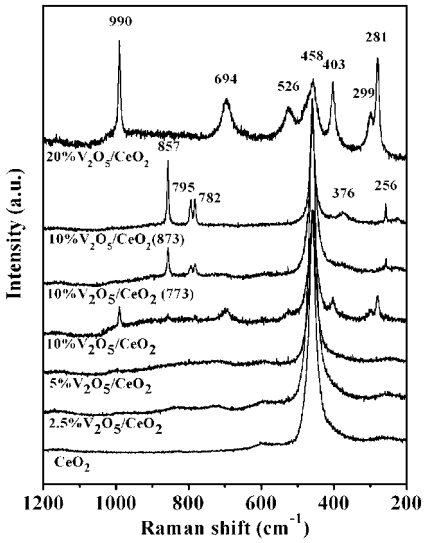

Fig. 3. Raman spectra of V_2O_5/CeO_2 catalysts. Samples were calcined at 673 K except for other two 10% V_2O_5/CeO_2 samples which were calcined at 773 and 873 K, respectively, as indicated.

In Fig. 3 are shown in the Raman spectra of CeO_2 and V_2O_5/CeO_2 catalysts. CeO_2 exhibits a characteristic Raman peak around 458 cm^{-1} [23,31], while crystalline V_2O_5 has the typical Raman peaks around 990, 694, 526, 403, 299 and 281 cm^{-1} [32]. The set of peaks at 857, 795, 782, 376 and 256 cm^{-1} belongs to $CeVO_4$ [23]. When the loading was low (2.5% and 5% V_2O_5), the Raman spectra only showed the peak for CeO_2, revealing the highly dispersed state of vanadium species in these two samples. Raman peaks for crystalline V_2O_5 appeared in the 10% V_2O_5/CeO_2, indicating that the amount of V_2O_5 in this sample exceeded the monolayer capacity. The 20% V_2O_5/CeO_2 sample exhibited intensive Raman peaks for the crystalline V_2O_5. Wachs and coworker [13] suggested a SVD of 8 V/nm^2 for the monolayer dispersion of vanadia over CeO_2, which was coincident with our value measured (8.02 V/nm^2) for the 10% V_2O_5/CeO_2. It should be mentioned that the XRD pattern did not show any sign for the presence of crystalline V_2O_5 in the 10% V_2O_5/CeO_2. Instead, the XRD clearly indicated the presence of $CeVO_4$ in the 10% V_2O_5/CeO_2, while the Raman spectrum only showed a very weak peak for $CeVO_4$ in this sample. This is a case that indicates the advantage to use different techniques for the determination of surface structures of vanadium species. With the increase of calcination temperature, the Raman peaks for $CeVO_4$ became more intensive while those for crystalline V_2O_5 disappeared. This result indicated the diffusion of vanadium cations into the lattice of CeO_2 and the formation of more $CeVO_4$ on the surface with the increase of calcination temperatures.

XPS spectra for the 10% V_2O_5/CeO_2 are shown in Figs. 4 and 5. The corresponding binding energies and surface V/Ce atomic ratios were summarized in Table 2. With the increase of calcination temperature, the binding energies for O 1s and Ce $3d_{5/2}$ were lowered, probably due to the formation of $CeVO_4$. In fact, cerium in $CeVO_4$ was in the valence of +3. Literature data showed that the binding energy for V^{5+} in V_2O_5

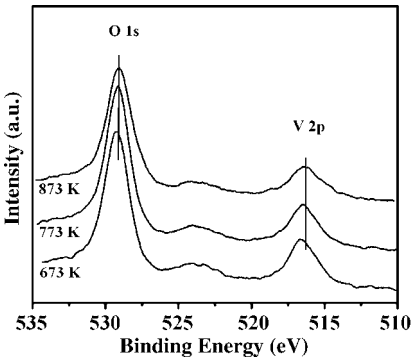

Fig. 4. XPS spectra of O 1s and V 2p in the 10% V_2O_5/CeO_2 catalyst calcined at different temperatures.

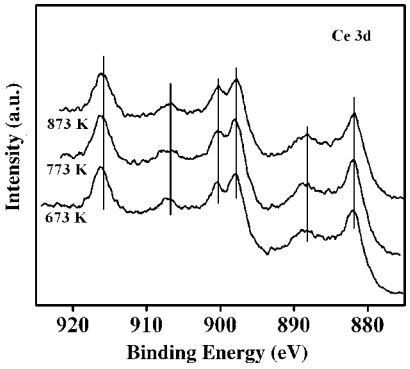

Fig. 5. XPS spectra of Ce 3d in the 10% V_2O_5/CeO_2 catalyst calcined at different temperatures.

was between 517.4 and 516.4 eV, while it was between 515.7 and 515.4 eV for V^{4+} in V_2O_4 [33]. With the increase of calcination temperature from 673 to 773 K, the binding energy of V $2p_{3/2}$ in 10% V_2O_5/CeO_2 decreased from 516.70 to 516.45 eV, indicating some extent of reduction of vanadium cations. Further increase of calcination temperature to 873 K did not bring about the further decrease of binding energy, probably due to the formation of $CeVO_4$, in which vanadium cations were in the valent state of +5. The surface V/Ce atomic ratio increased and then decreased with the increase of calcination temperature, revealing that vanadia spread further on the surface of CeO_2 and then diffused into the lattice of CeO_2.

3.2. Acid–base properties

Fig. 6 displays the results of microcalorimetric adsorption of NH_3 on CeO_2, V_2O_5 and the V_2O_5/CeO_2 catalysts at 423 K.

Table 2
Binding energies (eV) of O 1s, Ce $3d_{5/2}$, and V $2p_{3/2}$ as well as V/Ce atomic ratios for the 10% V_2O_5/CeO_2 catalyst calcined at different temperatures

Calcination temperature (K)	Binding energy (eV)			V/Ce atomic ratio
	O 1s	Ce $3d_{5/2}$	V $2p_{3/2}$	
673	529.20	882.10	516.70	0.44
773	529.15	882.00	516.45	0.47
873	529.10	881.75	516.45	0.31

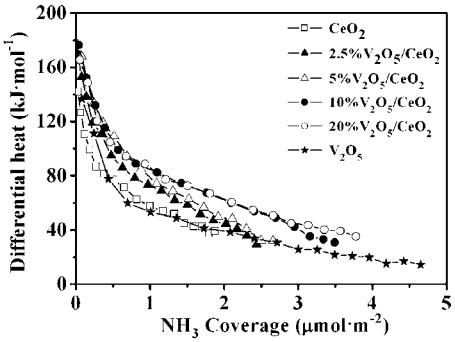

Fig. 6. Differential heats vs. coverage for NH_3 adsorption at 423 K on V_2O_5, CeO_2 and V_2O_5/CeO_2 catalysts.

The results showed that CeO_2 was quite acidic, with initial heat of 142 kJ/mol and coverage of 1.9 mol/m^2 for the adsorption of NH_3. Addition of V_2O_5 enhanced the surface acidity: the initial heat was 169 and 177 kJ/mol with the NH_3 coverage of 2.4 and 2.7 mol/m^2, respectively, for the 2.5% and 5% V_2O_5/CeO_2. The strong acid sites must be due to the highly dispersed vanadia since either CeO_2 or V_2O_5 alone displayed lower initial heat for ammonia adsorption. Similar results have been reported for V_2O_5/TiO_2 catalysts [17,18]. Further increase of loading of V_2O_5 did not bring about the further increase of initial heats, but increased the ammonia coverage significantly, indicating the formation of weak acidic sites. These weak acid sites might be due to the crystalline V_2O_5 that appeared when the loading exceeded the monolayer capacity for the 10% and 20% V_2O_5/CeO_2. Similar results were reported for V_2O_5/SiO_2 catalysts [17,18]. V_2O_5 usually does not spread on SiO_2. It forms crystalline grains on the surface of SiO_2 and creates weak acid sites. The surface area of V_2O_5 was low. Microcalorimetric adsorption of ammonia showed that the surface acid sites on V_2O_5 were not strong, but dense. The initial heat was 137 kJ/mol and the coverage was about 4.5 mol/m^2 for the adsorption of ammonia on unsupported V_2O_5.

The results of microcalorimetric adsorption of ammonia on the 10% V_2O_5/CeO_2 calcined at different temperatures were shown in Fig. 7. Although surface areas were decreased greatly after calcination at temperatures higher than 673 K, the initial heat and site density for ammonia adsorption did not decreased significantly. In fact, the initial heat and site density for the

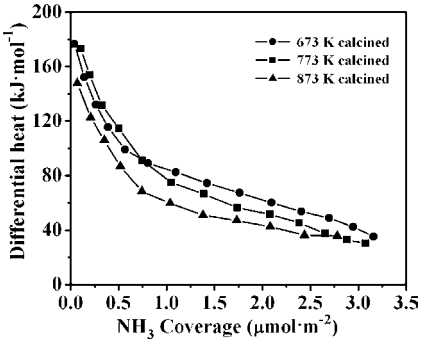

Fig. 7. Differential heats vs. coverage for NH_3 adsorption at 423 K on the 10% V_2O_5/CeO_2 calcined at 673, 773 and 873 K, respectively.

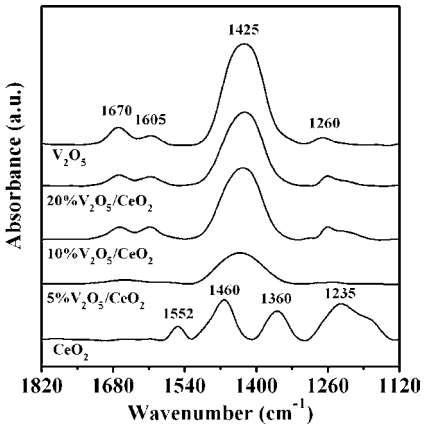

Fig. 8. FTIR spectra for NH_3 adsorption at room temperature on V_2O_5/CeO_2 catalysts.

samples calcined at 673 and 773 K were essentially the same, again indicating that these two samples might have similar surface structure. Only after calcination at 873 K, the initial heat and site density were decreased for ammonia adsorption.

FTIR spectra for ammonia adsorption on V_2O_5, CeO_2 and V_2O_5/CeO_2 samples were shown in Figs. 8 and 9. It is generally believed that the IR peaks around 1393, 1450, and 1680 cm^{-1} are due to the vibrations of NH_4^+ produced by the NH_3 adsorption on Brönsted acid sites, while the peaks around 1610 and 1230–1260 cm^{-1} are due to the coordinatively adsorbed NH_3 on Lewis acid sites [34,35]. We assigned the peaks at 1460 and 1360 cm^{-1} for Brönsted acid sites while those at 1552, 1235 cm^{-1} for Lewis acid sites on CeO_2. Thus, both Brönsted and Lewis acid sites were quite a few on CeO_2. On the other hand, V_2O_5 displayed mainly the Brönsted acidity with a main IR peak around 1425 cm^{-1}. The IR spectra of 5–20% V_2O_5/CeO_2 samples were similar to that of V_2O_5, clearly evidencing that the surface of CeO_2 was covered by V_2O_5. The IR spectrum for the 10% V_2O_5/CeO_2 calcined at 873 K still showed the main peak for Brönsted acid sites (Fig. 9), indicating that the surface of this sample was also mainly covered by vanadium species although both XRD and LRS demonstrated that the main species on the surface of this sample might be $CeVO_4$. The IR peaks at 1605 and 1260 cm^{-1} became weaker

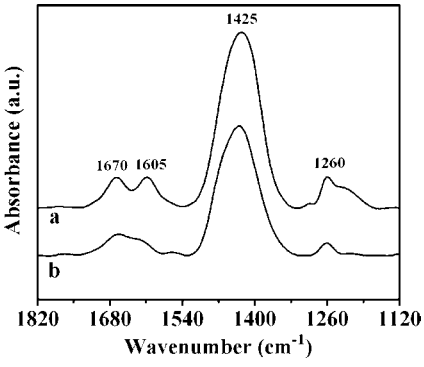

Fig. 9. FTIR spectra for NH_3 adsorption at room temperature on 10% V_2O_5/CeO_2 calcined at 673 K (a) and 873 K (b).

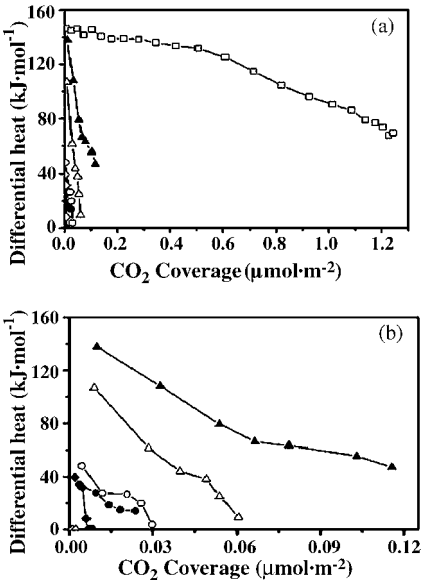

Fig. 10. Differential heats vs. coverage for CO_2 adsorption at 423 K on CeO_2 (□), 2.5% V_2O_5/CeO_2 (▲), 5% V_2O_5/CeO_2 (□), 10% V_2O_5/CeO_2 (●) and 20% V_2O_5/CeO_2 (○) calcined at 673 K as well as the 10% V_2O_5/CeO_2 calcined at 773 K (□) and at 873 K (□).

when calcined at higher temperature, indicating the diffusion of surface crystalline V_2O_5 into the lattice of CeO_2.

CeO_2 is an amphoteric compound, exhibiting both surface acidity and basicity. Fig. 10 presents the results for microcalorimetric adsorption of CO_2 at 423 K on CeO_2 and the V_2O_5/CeO_2 samples. CeO_2 exhibited the initial heat of 138 kJ/mol and site density of about 1.2 μmol/m^2 for CO_2 adsorption. Addition of even small amount of V_2O_5 (2.5%) greatly decreased the site density for CO_2 adsorption, indicating the well dispersion of V_2O_5 on the surface of CeO_2. With the further increase of loading of V_2O_5, the base sites as titrated by CO_2 continued to decrease up to 10% V_2O_5/CeO_2 with which surface crystalline V_2O_5 appeared. Calcination at temperatures higher than 673 K further decreased the surface sites for CO_2 adsorption, apparently owing to the formation of $CeVO_4$.

3.3. Redox properties

TPR is frequently used to study the redox property of metal oxide catalysts. Figs. 11 and 12 present the TPR results for V_2O_5, CeO_2 and V_2O_5/CeO_2 catalysts with different loadings and calcination temperatures. Although a detailed description of these TPR profiles is difficult, some useful information can still be obtained by observing the systematic changes of these profiles.

Fig. 11 shows that there were two TPR peaks around 715 and 833 K for CeO_2 at lower temperature region that can be attributed to the reduction of surface Ce^{4+} to Ce^{3+} [36]. The peaks with temperatures higher than 1100 K might be assigned to the reduction of bulk CeO_2 [36]. Addition of 2.5% V_2O_5 brought about the increase of the peak around 830 K, apparently owing to the reduction of surface vanadium species, and almost did not change the peaks for CeO_2 at the high temperature region. At the same time, the peak around 715 K for the

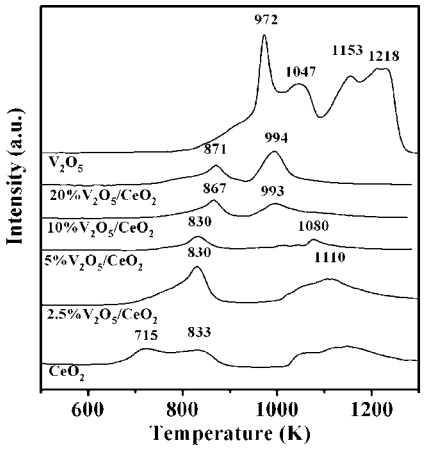

Fig. 11. TPR profiles of V_2O_5, CeO_2 and V_2O_5/CeO_2 catalysts.

reduction of surface CeO_2 was significantly decreased. Increase of loading to 5% led to more changes of the TPR profile: the peak at 715 K for surface CeO_2 disappeared and the unresolved peaks for bulk CeO_2 were diminished to a much smaller peak around 1080 K. Since 5% V_2O_5 is close to the monolayer capacity, this result indicates that covering CeO_2 surface by vanadium species inhibited the reduction of CeO_2 both on the surface and in the bulk. Thus, the peaks around 830 and 1080 K in the TPR profile of 5% V_2O_5/CeO_2 may be assigned to the reduction of surface vanadium species and bulk CeO_2, respectively. It appears that the reduction of surface vanadium species on CeO_2 was totally different from that of bulk V_2O_5. In fact, Fig. 11 shows that the TPR profile of our bulk V_2O_5 sample possessed four peaks around 972, 1047, 1153 and 1218 K, which was different from those reported in the literature [37,38].

10% and 20% V_2O_5/CeO_2 samples had the similar TPR profiles, with two peaks around 870 and 990 K. As compared to those of 2.5% and 5% V_2O_5/CeO_2, it is apparent that the low temperature peak shift to higher temperature while the high temperature peak shift to lower temperature in the TPR profiles of 10% and 20% V_2O_5/CeO_2. In addition, the area of the peak at the higher temperature increased significantly. We attributed the peak around 870 K to the reduction of surface vanadia while that around 990 K to the reduction of bulk CeO_2. This assignment was consistent with the results of structural characterizations as well as the TPR results for the 10% V_2O_5/CeO_2 calcined at different temperatures (Fig. 12).

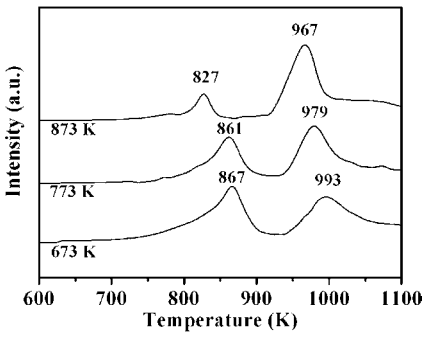

Fig. 12. TPR profiles of 10% V_2O_5/CeO_2 calcined at different temperatures.

Raman spectroscopy indicated the presence of crystalline V_2O_5 on the surface of 10% and 20% V_2O_5/CeO_2 samples. It is reasonable that the crystalline V_2O_5 particles exhibited reduction peak temperature higher than the highly dispersed vanadium species. Thus, the reduction peak around 870 K in the TPR profiles of 10% and 20% V_2O_5/CeO_2 can actually be assigned to the reduction of crystalline V_2O_5 with highly dispersed vanadium species on the surface. In addition, the two samples had the high loading of V_2O_5 and XRD results revealed the formation of $CeVO_4$. The formation of $CeVO_4$ could be facilitated during TPR process. Thus, the peak around 990 K in the TPR profiles of 10% and 20% V_2O_5/CeO_2 can be assigned to the reduction of bulk Ce^{4+} to Ce^{3+} with the formation of $CeVO_4$.

The TPR results from the 10% V_2O_5/CeO_2 calcined at different temperatures support the above assignments. It is seen from Fig. 12 that both peaks shift to lower temperatures with the increase of calcination temperature. In addition, the area of the peak at lower temperature became smaller. This may be explained as this. Increasing calcination temperature promoted the diffusion of vanadium cations into the lattice of CeO_2, which decreased the amount and size of surface crystalline V_2O_5 and thereby led to the lower reduction peak temperature and decreased peak area. No apparent peak area change can be observed for the peak at higher temperature. The peak also shifts to lower temperature, which might be due to the formation of $CeVO_4$ that facilitated the reduction of Ce^{4+} to Ce^{3+}.

3.4. Isopropanol probe reaction

The isopropanol (IPA) probe reaction has been extensively used to characterize the surface acid/base properties. It is generally true that IPA converts to propylene (PPE) and diisopropyl ether (DIPE) on acid sites while converts to acetone (ACE) on base sites when the reaction is performed in an inert atmosphere [39]. However, when the reaction is carried out with the presence of O_2, IPA can be oxidized to ACE, which may be used to characterize the redox property of a catalyst [40–42].

Table 3 and Fig. 13 present the results for the probe reaction of IPA on CeO_2, V_2O_5 and V_2O_5/CeO_2 catalysts in N_2 at 493 K. CeO_2 exhibited low activity for the reaction. Addition of V_2O_5 greatly enhanced the activity due to the increase of surface acidity (increased the selectivity to PPE and DIPE). The IPA conversion reached maximum at the loading (V_2O_5)

Table 3
Conversion of isopropanol on CeO_2, V_2O_5 and V_2O_5/CeO_2 catalysts in N_2 at 493 K

Catalyst	IPA conv. (%)	Sel. to PPE (%)	Sel. to DIPE (%)	Sel. to ACE (%)
CeO_2	0.6	76	0	24
2.5% V_2O_5/CeO_2	1.3	74	10	16
5% V_2O_5/CeO_2	4.6	58	34	8
10% V_2O_5/CeO_2	21.8	51	46	3
20% V_2O_5/CeO_2	7.0	48	44	8
V_2O_5	7.2	71	1	28

Note: IPA, PPE, DIPE and ACE represent isopropanol, propylene, diisopropyl ether and acetone, respectively.

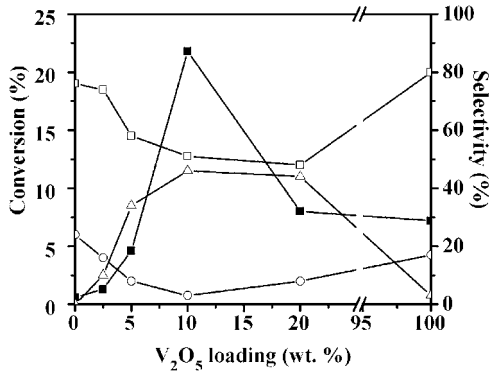

Fig. 13. Conversion of isopropanol (■) and selectivity to propylene (□), diisopropyl ether (□), and acetone (◯) on CeO_2, V_2O_5 and V_2O_5/CeO_2 catalysts in N_2 at 493 K.

of 10%. Then, the conversion of IPA decreased with the further increase of loading. This indicates that the addition of V_2O_5 with the loading significantly higher than the monolayer capacity could not lead to the high surface acidity. In contrast, high loading of V_2O_5 might cause the decrease of surface area and the formation of surface crystalline V_2O_5 and thus decreased the activity for the conversion of IPA. The selectivity to ACE decreased with the increase of V_2O_5 loading up to 10%. This can be explained by the gradual neutralization of surface basicity of CeO_2 by V_2O_5. Further increasing V_2O_5 loading, the selectivity to ACE increased again. This might be caused by the direct dehydrogenation of IPA on vanadium species [43]. In addition, the selectivity to PPE decreased while that to DIPE increased with the increase of V_2O_5 loading for the V_2O_5/CeO_2 catalysts. This result indicated that the formation of surface crystalline V_2O_5 might decrease the surface acidity, which is consistent with the results of microcalorimetric adsorption of ammonia presented above. It is generally believed that strong acid sites favor the dehydration in a molecule of IPA to form PPE while the weak acid sites favor the dehydration between two molecules of IPA to form DIPE.

Table 4 gives the results of IPA probe reaction in N_2 for the 10% V_2O_5/CeO_2 calcined at different temperatures. The conversion of IPA at 413 K on these samples was high enough for a comparison. Since the reaction temperature is relatively low, DIPE was the main reaction product (>90%). The results in Table 4 showed that the 10% V_2O_5/CeO_2 calcined at 673 and 773 K exhibited similar surface acidity for the conversion of IPA. Calcination at 873 K greatly decreased the IPA conversion, reflecting the decreased surface acidity. These results agree well

Table 4
Conversion of isopropanol in N_2 at 413 K on the 10% V_2O_5/CeO_2 catalysts calcined at different temperatures

Catalyst	IPA conv. (%)	Sel. to PPE (%)	Sel. to DIPE (%)	Sel. to ACE (%)
10% V_2O_5/CeO_2 (673 K)	6.1	6	92	2
10% V_2O_5/CeO_2 (773 K)	7.8	5	95	0
10% V_2O_5/CeO_2 (873 K)	0.8	8	92	0

Note: IPA, PPE, DIPE and ACE represent isopropanol, propylene, diisopropyl ether and acetone, respectively.

Table 5
Conversion of isopropanol in air at 393 K on CeO_2, V_2O_5 and V_2O_5/CeO_2 catalysts

Catalyst	IPA conv. (%)	Sel. to PPE (%)	Sel. to DIPE (%)	Sel. to ACE (%)
CeO_2	0.3	9	0	91
2.5% V_2O_5/CeO_2	4.5	1	2	97
5% V_2O_5/CeO_2	4.6	1	0	99
10% V_2O_5/CeO_2	3.2	5	2	93
10% V_2O_5/CeO_2 (773 K)	3.0	2	6	92
10% V_2O_5/CeO_2 (873 K)	1.1	4	0	96
20% V_2O_5/CeO_2	4.6	13	35	52
V_2O_5	7.8	25	52	23

Note: IPA, PPE, DIPE and ACE represent isopropanol, propylene, diisopropyl ether and acetone, respectively.

with the surface acidity for the samples as measured by the microcalorimetric adsorption of ammonia.

Table 5 presents the results for the probe reaction of IPA on CeO_2, V_2O_5 and V_2O_5/CeO_2 catalysts in air at 393 K. The presence of O_2 greatly enhanced the conversion of IPA as well as the selectivity to acetone, an oxidative dehydrogenation product, indicating that the redox process over these catalysts underwent easily for the probe reaction. Although the surface area of V_2O_5 was much lower than that of CeO_2, it exhibited much higher activity than CeO_2 for the selective oxidation of IPA. This demonstrates that V_2O_5 possesses stronger redox ability than CeO_2. The product selectivity showed that CeO_2 exhibited mainly redox property with acetone as its main product while V_2O_5 displayed acidic property with the formation of mainly dehydration products.

Addition of 2.5% and 5% V_2O_5 on CeO_2 greatly enhanced the conversion of IPA. The selectivity to acetone was also increased. Such result suggests that the vanadium species highly dispersed on CeO_2 was of strong redox ability and displayed little surface acidity for the IPA probe reaction with the presence of O_2. Further increase of loading (V_2O_5) to 10% resulted in an increase of selectivity to propylene and a decrease of selectivity to acetone, indicating the increase of surface acidity owing to the formation of crystalline V_2O_5 in the 10% V_2O_5/CeO_2 (Raman result). The catalyst with 20% V_2O_5 exhibited significant surface acidity with 48% dehydration products. In fact, this sample possessed significant amount of crystalline V_2O_5 particles on the surface (Raman and XRD results).

The 10% V_2O_5/CeO_2 calcined at different temperatures showed the similar selectivity for the IPA probe reaction with the presence of O_2. They exhibited mainly the redox property with acetone as the main product. Increase of calcination temperature decreased the conversion of IPA. It is interesting to note that the 10% V_2O_5/CeO_2 (673 K) and 10% V_2O_5/CeO_2 (773 K) exhibited similar conversion and selectivity for the IPA probe reaction. This indicates that although the structural characterizations showed some differences in surface phases in the two samples, the main surface structure of the two samples might be essentially the same, leading to the similar surface acidity and redox property. The active sites in this case might be the highly dispersed vanadium species in the two samples. Structural

Table 6
Results of selective oxidation of toluene on CeO_2, V_2O_5 and V_2O_5/CeO_2 catalysts at 623 K

Catalyst	Tolue conv. (%)	Sel. to BAo (%)	Sel. to BA (%)	Sel. to BAc (%)	Sel. to COx (%)	Total sel. (%)	Total yield (%)
CeO_2	20.9	0	0	0	100	0	0
2.5% V_2O_5/CeO_2	25.0	0	17.3	0	82.7	17.3	4.3
5% V_2O_5/CeO_2	24.7	0.7	17.8	0.2	81.3	18.7	4.6
10% V_2O_5/CeO_2	21.4	0	18.4	0	81.6	18.4	3.9
10% V_2O_5/CeO_2 (773 K)	22.4	0.6	14.0	1.0	84.4	15.6	3.5
10% V_2O_5/CeO_2 (873 K)	4.0	2.7	59.6	0	37.7	62.3	2.5
20% V_2O_5/CeO_2	23.5	0.6	13.5	0.3	85.6	14.4	3.4
V_2O_5	4.2	0	52	0	46	52	2.2

Note: Tolue, BAo, BA and BAc denote toluene, benzyl alcohol, benzaldehyde and benzoic acid, respectively.

characterizations showed that the surface of 10% V_2O_5/CeO_2 (873 K) was mainly covered by $CeVO_4$. It exhibited low conversion of IPA even with the presence of O_2. But the selectivity to acetone was increased as compared to the other two counterparts. Thus, this sample possessed low surface acidity and weak redox ability, but its redox ability did not seem to be decreased as much as its acidity.

3.5. Selective oxidation of toluene

Table 6 gives the results for the selective oxidation of toluene over CeO_2, V_2O_5 and V_2O_5/CeO_2 catalysts at 623 K. Only non-selective reactions occurred on CeO_2, and V_2O_5 was not active at all at 623 K for the reaction. All the V_2O_5/CeO_2 catalysts calcined at 673 K exhibited similar conversion of toluene (21–25%), and the catalysts containing 2.5–10% V_2O_5 (673 K calcination) showed the similar selectivity to benzaldehyde (17–18%). Structural characterizations above showed that the 2.5% and 5% V_2O_5/CeO_2 possessed exclusively while the 10% V_2O_5/CeO_2 (673 K) mainly the highly dispersed vanadium species on the surface. Only small amount of crystalline V_2O_5 were present on the surface of 10% V_2O_5/CeO_2 (673 K). In addition, these samples exhibited similar catalytic behavior for the IPA probe reaction with the presence of O_2. Thus, the similar surface structure as well as the similar surface acidity and redox property might be responsible for the similar behavior of these catalysts for the selective oxidation of toluene. The 20% V_2O_5/CeO_2 catalyst possessed significant amount of crystalline V_2O_5 on the surface and exhibited significant surface acidity in the IPA probe reaction even with the presence of O_2. Thus, the sample exhibited lower selectivity to benzaldehyde for the oxidation of toluene. It was known that the surface of 10% V_2O_5/CeO_2 (873 K) was mainly covered by $CeVO_4$, displaying weak surface acidity and a relatively stronger redox property in the IPA probe reaction with the presence of O_2. Accordingly, this catalyst exhibited low toluene conversion (4%), but significantly enhanced selectivity to benzaldehyde (∼60%). Although the catalysts 2.5–10% V_2O_5/CeO_2 (673 K) exhibited mainly the redox property for the IPA probe reaction with the presence of O_2, they showed mainly the surface acidity for the IPA probe reaction in N_2. That might be why the selectivity to benzaldehyde over these catalysts was low. In contrast, the 10% V_2O_5/CeO_2 (873 K) showed low surface acidity even for the IPA probe reaction in N_2.

A few types of surface species may exist when V_2O_5 is dispersed on CeO_2 [44]. These surface species may involve the following: (1) isolated VO_4 unit, (2) dimeric or polymeric vanadium species, (3) two-dimensional network of vanadium species, (4) three-dimensional crystalline V_2O_5 and (5) $CeVO_4$, a product of solid phase reaction. Structural characterizations showed that in the catalysts studied in this work, the 2.5% and 5% V_2O_5/CeO_2 might have dimeric or polymeric vanadium species on the surface. In the 10% V_2O_5/CeO_2 sample, there might be the two-dimensional network of vanadium species on the surface since the amount of vanadia in this sample exceeded the monolayer capacity. Some crystalline V_2O_5 and $CeVO_4$ were also observed in this sample. Significant amount of three-dimensional crystalline V_2O_5 were present in the 20% V_2O_5/CeO_2 sample. Calcination at temperatures higher than 673 K resulted in the formation of significant amount of $CeVO_4$.

There might be three types of V–O bonds in the supported V_2O_5 catalysts, i.e. V=O, V–O–V and V–O-support [44]. Dumesic and coworker suggested the formation of V–OH (surface acid sites) from V=O [16]. The density of V–OH increases with the increase of loading up to the monolayer capacity when it reaches maximum. This trend was observed in our IPA probe reactions for the V_2O_5/CeO_2 catalysts. The redox property of the catalysts might be mainly originated from the bonds V–O-support instead of the V–O–V bonds. This is because that bulk V_2O_5 exhibited mainly the acidic rather than the redox property. Weckhuysen and Keller [44] ascribed the activity of selective oxidation of methanol to formaldehyde to the V–O-support bonds in the supported vanadia catalysts after comparing the effects of different supports. Christodoulakis et al. [45] also found that the V–O-support bonds played an important role in the supported vanadia catalysts for the dehydrogenation of propane. It is difficult to determine the surface density of the V–O-support bonds directly. However, it is reasonable to infer that the highest density of the surface V–O-support bonds might be reached when the loading of V_2O_5 is lower than the monolayer capacity, since once the loading reaches the monolayer capacity, the surface vanadium species would form a two-dimensional network in which V–O–V may be the most popular bonds. The V_2O_5 loading in the 5% V_2O_5/CeO_2 was close to the monolayer capacity as discussed above. This catalyst might possess strongest redox ability in the catalysts studied here. In fact, it exhibited the

highest activity for the selective oxidation of IPA and toluene. The so-called highly dispersed vanadium species we mentioned above can be taken as the isolated, dimeric and polymeric vanadium species. The surface V–O–Ce bonds seemed important for the selective oxidation of toluene. However, once $CeVO_4$ was formed, the activity for the oxidation reactions decreased. It seemed that the oxygen anions in $CeVO_4$ were less active than those in CeO_2 and V_2O_5 since they were more strongly bonded in the lattice of $CeVO_4$ than in those of CeO_2 and V_2O_5. The reason may be simple. The valent states of Ce and V are relatively stabilized at +3 and +5, respectively, in $CeVO_4$, leading to the weakened redox ability of $CeVO_4$. Therefore, the catalyst with abundant surface $CeVO_4$ exhibited low activity for the oxidation of toluene, but high selectivity to benzaldehyde.

4. Conclusion

In conclusion, we demonstrated in this work that V_2O_5 can be well dispersed on the surface of CeO_2. The monolayer dispersion capacity was found to be about 8 V/nm^2, corresponding to about 10% V_2O_5 by weight in a V_2O_5/CeO_2 sample with the surface area of about 80 m^2/g. Variation of loading of V_2O_5 and calcination temperature brought about the changes of surface structures of dispersed vanadium species, and hence the surface acidic and redox properties. Microcalorimetric adsorption of NH_3 and CO_2 indicated that CeO_2 possessed fairly strong surface acidity and basicity. Addition of V_2O_5 enhanced the surface acidity as well as the redox property, but decreased the surface basicity. Isopropanol was mainly converted to dehydration products (propylene and diisopropyl ether) without O_2, while mainly to oxidation product (acetone) with O_2, over the V_2O_5/CeO_2 catalysts. However, V_2O_5 and the 20% V_2O_5/CeO_2 catalyst exhibited surface acidity with the formation of significant amount of dehydration products in the isopropanol probe reaction even performed with the presence of O_2. The combination of the reactions for the conversions of isopropanol with and without the presence of O_2 seems to probe the variations of surface structure, acidity and redox property of the V_2O_5/CeO_2 catalysts sensitively. The probe reaction revealed that vanadium species were highly dispersed on the surface of the V_2O_5/CeO_2 catalysts with loading lower than 10%, although structural characterizations (XRD and LRS) indicated the presence of small amount of phases such as crystalline V_2O_5 and $CeVO_4$ in the 10% V_2O_5/CeO_2. The 20% V_2O_5/CeO_2 catalyst possessed significant amount of crystalline V_2O_5 on the surface and therefore it exhibited catalytic properties similar to bulk V_2O_5 for the probe reaction. Calcination of the 10% V_2O_5/CeO_2 catalyst at 873 K resulted in the formation of mainly $CeVO_4$ on the surface, which showed low surface acidity and redox ability. However, the probe reaction indicated that the calcination at 873 K seemed to cause the decrease of surface acidity more than redox ability. Thus, it exhibited much higher selectivity to benzaldehyde as compared to the other V_2O_5/CeO_2 catalysts studied in this work, although its activity for the conversion of toluene was low.

Acknowledgements

We acknowledge the financial supports from NSFC (20373023), NSFC-SINOPEC (20233040) and PRA-E0301.

References

[1] F. Roozenboom, P.D. Cordingley, P.J. Gellings, J. Catal. 68 (1981) 464.
[2] P. Forzatti, E. Tronconi, G. Busca, P. Tittarelli, Catal. Today 1 (1987) 209.
[3] M.S. Wainwright, N.R. Foster, Catal. Rev. Sci. Eng. 19 (1979) 211.
[4] V. Nikolov, D. Kissurski, A. Anastasov, Catal. Rev. Sci. Eng. 33 (1991) 319.
[5] P. Cavalli, F. Cavani, I. Manenti, F. Trifirò, Catal. Today 1 (1987) 245.
[6] M. Sanati, A. Andersson, J. Mol. Catal. 59 (1990) 233.
[7] J.N. Armor, Appl. Catal. B 1 (1992) 221.
[8] J.P. Dunn, P.R. Koppula, H.G. Stenger, I.E. Wachs, Appl. Catal. B 19 (1998) 103.
[9] H. Bosch, F. Janssen, Catal. Today 2 (1988) 39.
[10] C.N. Satterfield, Heterogeneous Catalysis in Practice, McGraw-Hill, New York, 1980.
[11] G.C. Bond, S.F. Tahir, Appl. Catal. 71 (1991) 1.
[12] I.E. Wachs, Chem. Eng. Sci. 45 (1990) 2561.
[13] L.J. Burcham, I.E. Wachs, Catal. Today 49 (1999) 467.
[14] G.T. Went, S.T. Oyama, A.T. Bell, J. Phys. Chem. 94 (1990) 4240.
[15] A. Khodakov, B. Olthof, A.T. Bell, E. Iglesia, J. Catal. 181 (1999) 205.
[16] T. Kataoka, J.A. Dumesic, J. Catal. 112 (1988) 66.
[17] M. Li, J. Shen, J. Catal. 205 (2002) 248.
[18] H. Zou, M. Li, J. Shen, A. Auroux, J. Therm. Anal. Calorim. 72 (2003) 209.
[19] F. Arena, F. Frusteri, A. Parmaliana, Appl. Catal. A 176 (1999) 189.
[20] A. Trovarelli, Catal. Rev. Sci. Eng. 38 (1996) 439.
[21] S. Bernal, F.J. Botana, J.J. Calvino, G.A. Cifredo, J.A. Pérez-Omil, J.M. Pintado, Catal. Today 23 (1995) 219.
[22] R. Cousin, M. Dourdin, E. Abi-Aad, D. Courcot, S. Capelle, M. Guelton, A. Aboukaïs, J. Chem. Soc., Faraday Trans. 93 (1997) 3863.
[23] J. Matta, D. Courcot, E. Abi-Aad, A. Aboukaïs, Chem. Mater. 14 (2002) 4118.
[24] W. Daniell, A. Ponchel, S. Kuba, F. Anderle, T. Weingand, D.H. Gregory, H. Knözinger, Top. Catal. 20 (2002) 65.
[25] S.T. Oyama, G.T. Went, K.B. Lewis, A.T. Bell, G.A. Somorjai, J. Phys. Chem. 93 (1989) 6786.
[26] F.E. Massoth, Adv. Catal. 27 (1978) 265.
[27] F. Roozeboom, M.C. Mittelmeijer-Hazeleger, J.A. Moulijn, J. Medma, V.H.J. de Beer, P.J. Gellings, J. Phys. Chem. 84 (1980) 2783.
[28] B.S. Parekh, S.W. Weller, J. Catal. 47 (1977) 100.
[29] S.W. Weller, Acc. Chem. Res. 16 (1983) 101.
[30] B.M. Reddy, B. Manohar, E.P. Reddy, Langmuir 9 (1993) 1781.
[31] P. Fornasiero, G. Balducci, R. Di Monte, J. Kašpar, V. Sergo, G. Gubitosa, A. Ferrero, M. Graziani, J. Catal. 164 (1996) 173.
[32] E.C. Alyea, L.J. Lakshmi, Z. Ju, Langmuir 13 (1997) 5621.
[33] V.I. Bukhtiyarov, Catal. Today 56 (2000) 403.
[34] J. Shen, R.D. Cortright, Y. Chen, J.A. Dumesic, J. Phys. Chem. 98 (1994) 8067.
[35] H. Knözinger, Adv. Catal. 25 (1976) 184.
[36] A. Trovarelli, G. Dolcetti, C. de Leitenburg, J. Kašpar, P. Finetti, A. Santoni, J. Chem. Soc., Faraday Trans. 88 (1992) 1311.
[37] M.M. Koranne, J.G. Goodwin Jr., G. Marcelin, J. Catal. 148 (1994) 369.
[38] E.P. Reddy, R.S. Varma, J. Catal. 221 (2004) 93.
[39] A. Gervasini, J. Fenyvesi, A. Auroux, Catal. Lett. 43 (1997) 219.
[40] D. Haffad, A. Chambellan, J.C. Lavalley, J. Mol. Catal. A 168 (2001) 153.
[41] D. Kulkarni, I.E. Wachs, Appl. Catal. A 237 (2002) 121.
[42] X. Gu, H. Chen, J. Shen, Chin. J. Catal. 24 (2003) 885.
[43] X. Liu, X. Gu, J. Shen, Chin. J. Catal. 24 (2003) 674.
[44] B.M. Weckhuysen, D.E. Keller, Catal. Today 78 (2003) 25.
[45] A. Christodoulakis, M. Machli, A.A. Lemonidou, S. Boghosian, J. Catal. 222 (2004) 293.